Since January 2020 Elsevier has created a COVID-19 resource centre with free information in English and Mandarin on the novel coronavirus COVID-19. The COVID-19 resource centre is hosted on Elsevier Connect, the company's public news and information website.

HOSTED BY

ELSEVIER

CrossMark

Available online at www.sciencedirect.com

ScienceDirect

Radiology of Infectious Diseases 1 (2015) 51−56

www.elsevier.com/locate/jrid

Research article

Chest imaging of H7N9 subtype of human avian influenza

Xi-ming Wang [a], Su Hu [a,*], Chun-hong Hu [a,*], Xiao-yun Hu [b], Yi-xing Yu [a], Ya-fei Wang [c], Jian-liang Wang [d], Guo-hua Li [e], Xin-feng Mao [f], Jian-chun Tu [g], Ling Chen [h], Wei-feng Zhao [i,*]

[a] *Imaging Centre, The First Affiliated Hospital of Soochow University, Suzhou, Jiangsu, 215006, China*
[b] *Department of Radiology, Wuxi Peoples' Hospital, Wuxi, Jiangsu, 214023, China*
[c] *Department of Radiology, Zhenjiang No 1 People' Hospital, Zhenjiang, Jiangsu, 212002, China*
[d] *Department of Radiology, Kunshan No 1 People' Hospital, Suzhou, Jiangsu, 215300, China*
[e] *Department of Radiology, Changshu City Hospital of Traditional Chinese Medicine, Suzhou, Jiangsu, 215500, China*
[f] *Department of Radiology, Huzhou Central Hospital, Huzhou, Zhejiang, 313000, China*
[g] *Department of Radiology, Kunshan City Hospital of Traditional Chinese Medicine, Suzhou, Jiangsu, 215300, China*
[h] *Department of Radiology, No 1 People' Hospital of Wujiang, Suzhou, Jiangsu, 215200, China*
[i] *Department of Infectious Diseases, The First Affiliated Hospital of Soochow University, Suzhou, Jiangsu, 215006, China*

Received 14 October 2014; accepted 6 January 2015
Available online 28 February 2015

Abstract

Background: Human infection with avian influenza A H7N9 virus is an acute respiratory infectious disease, which usually causes severe pneumonia with a high mortality. Chest radiographs and Computed Tomography (CT) are principal radiological modalities to assess the lung abnormalities.
Objectives: The goal of this study was to investigate the chest images characteristic of H7N9 subtype of human avian influenza.
Materials and methods: The clinical and imaging data of 11 cases diagnosed as H7N9 subtype of human avian influenza were collected from 4 cities in the southern region of the Yangtze River, China. The chest imaging manifestations were analyzed by the assigned expert group. The analyzed cases include 7 males and 4 females aged from 20 to 84 years, with a mean of 55.6 years. The clinical symptoms were mainly fever (100%, 11/11) and cough (72.7%, 8/11).
Results: Segmental or lobar ground-glass opacity (GGO) or consolidation was shown in 8 cases (72.7% or 8/11). Air bronchogram was found in 7 cases (63.6% or 7/11). The lesions developed into multiple or diffuse in both lungs rapidly at the progressive stage. The reticulation shadows were shown after some lesions absorbed at the stable stage.
Conclusions: The characteristic imaging demonstrations of H7N9 subtype of human avian influenza are segmental or lobar exudative lesions at lungs at the initial stage, which rapidly progress into bilateral distribution at lungs at the progressive stage.

Keywords: Human avian influenza; H7N9; Radiography; Tomography; Computed X-ray

1. Introduction

Human infection with avian influenza A H7N9 virus is an acute respiratory infectious disease. It firstly emerged in Anhui Province and Shanghai City, P.R. China in February, 2013 [1], and more cases were then reported in the Eastern China [2]. The disease is characterized by acute onset and high mortality, which poses a great threat to human health. In this paper, we

Abbreviations: CT, Computed Tomography; RT-PCR, real-time reverse transcriptase polymerase chain reaction; WBC, white blood cell count; GGO, ground-glass opacity; ARDS, acute respiratory distress syndrome; SARS, severe acute respiratory syndromes.

* Corresponding authors. Tel.: +86 512 67166217; fax: +86 512 65228072.
E-mail addresses: husu1022@126.com (S. Hu), hch5305@163.com (C.-h. Hu), szzhaoweifeng@aliyun.com (W.-f. Zhao).

Peer review under responsibility of Beijing You'an Hospital affiliated to Capital Medical University.

http://dx.doi.org/10.1016/j.jrid.2015.02.001

retrospectively reviewed chest radiographs and Computed Tomography (CT) findings in 11 patients that had confirmatively been diagnosed with H7N9 subtype of human avian influenza.

2. Materials and methods

2.1. Subjects

This study retrospectively reviewed the clinical and imaging data of 11 patients with H7N9 subtype of human avian influenza (Table 1) from 4 cities in the southern region of the Yangtze River, China. The diagnostic criteria of human infection with avian influenza A H7N9 virus was established by the National Health and Family Planning Commission of China (formerly Ministry of Health). The results of real-time reverse transcriptase polymerase chain reaction (RT-PCR) of nasal swabs and aspirates of all the 11 patients were positive for H7N9 avian influenza virus. All patients were approved by the expert board of Provicial Department of Health in Jiangsu or Zhejiang, China.

The study subjects included 7 males and 4 females with their ages ranging from 20 to 84 years and a mean of 55.6 years. All 11 patients had initially presented with influenza-like sympotoms, including fever (100%, 11/11), cough (72.7%, 8/11), expectoration (45.5%, 5/11), chest tightness (18.2%, 2/11), muscular pain (18.2%, 2/11), shortness of breath (9.1%, 1/11), fatigue (9.1%, 1/11), sore throat (9.1%, 1/11) and vomiting (9.1%, 1/11). Seven of the 11 subjects had the following medical histories: thoracic surgery with excision of thymoma($n = 1$), pregnancy($n = 1$), hypertension($n = 3$) and chronic bronchitis($n = 2$). The other 4 patients had no significant medical history. The initial WBC count was normal in 7 patients, low in 3 patients and high in 1 patient.

After onset of the illness, all 11 patients were hospitalized for 1–10 days and received antiviral and respiratory support therapies.

2.2. Imaging technologies

Posteroanterior radiographs were obtained using Axiom Aristos (Siemens Healthcare) with a constant technique of 125Kv and automatic mA adjustment. MDCT was performed on 64-MDCT scanner (Somatom Sensation, Siemens healthcare), 128-MDCT scanner (Somatom Definition, Siemens healthcare) and 4-MDCT scanner (Brightspeed excel, GE healthcare). The scan protocol was as the following: 120 kV, automatic mA adjustment (about 115mAs), pitch of 0.9, matrix of 512 × 512, thickness of 5.0–6.0 mm, interval of 1.4 mm, and 0.75 mm reformation.

All 11 patients had serial bedside anteroposterior-projection follow-up radiographs at an interval of 2 or 3 days, while only 7 patients required follow-up CT scans. Bedside anteroposterior-projection radiographs were obtained with a mobile unit (Philips Healthcare), using a standard exposure factor of 80 kV and 5 mAs.

2.3. Image analysis

The chest radiographs and MDCT images were independently reviewed by two experienced radiologists and final interpretations were achieved by consensus. The anatomic distribution was characterized as either unilateral or bilateral. The extent of abnormality was graded as focal, multifocal and diffuse. The abnormalities were characterized as consolidation (opacification with obscuration of the underlying vessels), ground-glass opacity (GGO) which increased attenuation without obscuration of the underlying vessels, nodules opacities and reticulation. The presence of enlarged lymph nodes and pleural effusions were also recorded.

3. Results

3.1. Initial image findings

The initial chest radiographs were abnormal in all 11 patients (Table 2) (Fig. 1A). The lung abnormalities were unilateral in 45.5% or 5/11 patients (4/5 in left lung and 1/5 in right lung) and bilateral in the rest of 6 patients. The abnormalities were found in one lobe in 4 patients, two lobes in 2 patients, three lobes in 2 patients and four lobes in 3 patients, respectively.

Table 1
Summary of the clinical data and initial examination of the 11 patients with H7N9 subtype of human avian influenza.

Case	Gender	Age (year)	Onset symptoms	Temperature (°C)	WBC ($\times 10^9$/L)	Interval between initial imaging exam and onset(d)	
						Radiograph	CT
1	F	32	Fever, cough, sputum	39.6	2.0	4	4
2	M	72	Fever, vomiting	39	6.2	3	3
3	F	20	Fever, cough, sputum	39	3.8	1	3
4	M	84	Fever, cough, sputum	39	5.27	6	3
5	M	72	Fever, cough, chest tightness,fatigue	39.4	7.42	7	7
6	M	60	Fever, chest tightness, shortness of breath,pharyngalgia	39.6	4.1	10	10
7	M	56	Fever, muscle ache	39.5	11.19	6	6
8	M	70	Fever, cough	38.6	4.7	9	16
9	F	25	Fever, cough, sputum, muscle ache	39.9	7.9	1	8
10	M	65	Fever, cough	38.6	7.0	4	3
11	F	56	Fever, cough,sputum	39.4	2.6	4	16

Table 2
Summary of the initial radiograph and CT scan in 11 patients with H7N9 subtype of human avian influenza.

Case	X-ray	CT
1	Unilateral patchy GGO	Unilateral segmental GGO
2	Unilateral patchy GGO	Unilateral segmental GGO
3	Bilateral patchy GGO	Bilateral lobar consolidation and nodular consolidation
4	Bilateral lobar consolidation	Bilateral lobar consolidation
5	Unilateral patchy consolidation	Unilateral segmental consolidation
6	Unilateral patchy consolidation	Unilateral segmental consolidation
7	Unilateral patchy consolidation	Unilateral segmental consolidation
8	Unilateral lobar consolidation	Bilateral lobar consolidation or GGO and nodular consolidation
9	Bilateral patchy consolidation and GGO	Bilateral segmental GGO and consolidation
10	Unilateral lobar consolidation	Bilateral lobar or segmental consolidation and nodular consolidation
11	Unilateral lobar consolidation	Bilateral patchy consolidation

The predominant chest imaging finding was segmental or lobar consolidation (72.7% or 8/11), among which three (3/8) showed multi-nodular opacities (Fig. 2A), and two (2/8) presented with combined segmental ground-glass opacity. Segmental ground-glass opacity was demonstrated in 2 patients (18.2% or 2/11). Multi-patchy shadows presented in 1 patient (9.1% or 1/11).

Air bronchogram was a commonly seen lung abnormality (63.6% or 7/11). A sharp boundary due to the interlobar fissure was also manifested (36.4% or 4/11).

Thickened adjacent pleura could be seen in four patients and pleural effusions were found in two patients. Lymph node enlargement was not significant in any of the eleven cases.

3.2. Follow-up imaging findings

During 3−15 days after onset, eight patients showed obvious progress of the conditions compared to initial abnormalities (Fig. 1B). Firstly, lesions increased in size, progress from unilateral to bilateral lungs or diffuse distribution (Fig. 2B). Secondly, density of abnormalities developed from GGO to consolidation. The patients at this stage were characterized as acute respiratory distress syndrome (ARDS), with occurrence of death in 2 cases and no obvious change in other 3 cases.

After 15 days, three of the rest 9 patients (3/9) were improved compared with the former lesions (Fig. 2C−2D). The abnormalities demonstrated as reticulation with a decreased extent. One of these three patients had segmental consolidation in the left upper lobe and segmental consolidation in bilateral lower lobes at the initial scanning, but was improved afterwards. One patient (1/9) who had previously undergone thoracic surgery for excision of thymoma showed segmental consolidation in the left upper lobe by the initial radiograph and CT scan seven days after onset (Fig. 3A), and diffuse GGO and consolidation at both lungs by the bedside radiograph ten days after onset (Fig. 3B). The extent and density of the abnormalities remained unchanged during the following twenty days (Fig. 3C−3D). The extent of abnormalities of the other five patients also remained unchanged but with invariable or slightly deteriorated clinical conditions. Death occurred in another 4 cases at this stage.

4. Discussion

On March 2013, a subtype of avian influenza virus causing human infections, H7N9, was identified in Eastern China. H7 subtypes (H7N2, H7N3 and H7N7) of avian influenza viruses are commonly found and are often limited to mild illness, among which only one case of death was reported in

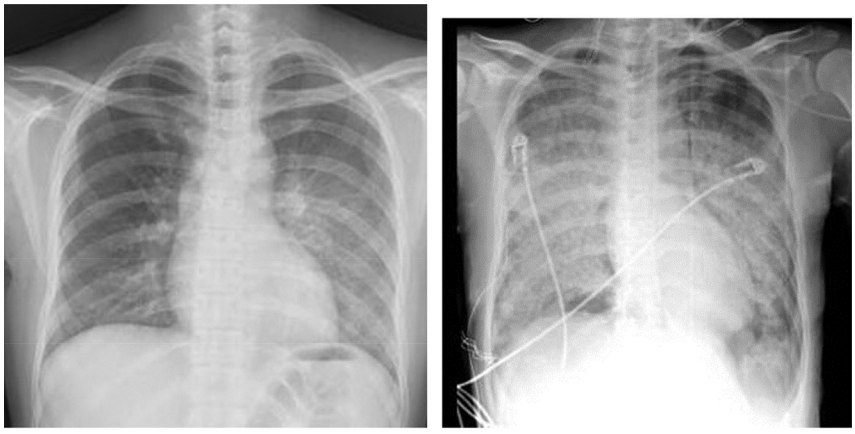

A B

Fig. 1. 32-year-old female patient with H7N9 subtype of human avian influenza. A. Chest radiograph obtained at d 4 after onset shows patchy ground-glass opacities in left lung. B. Bedside chest radiograph obtained at d 6 after A shows bilateral diffuse consolidation and ground-glass opacities.

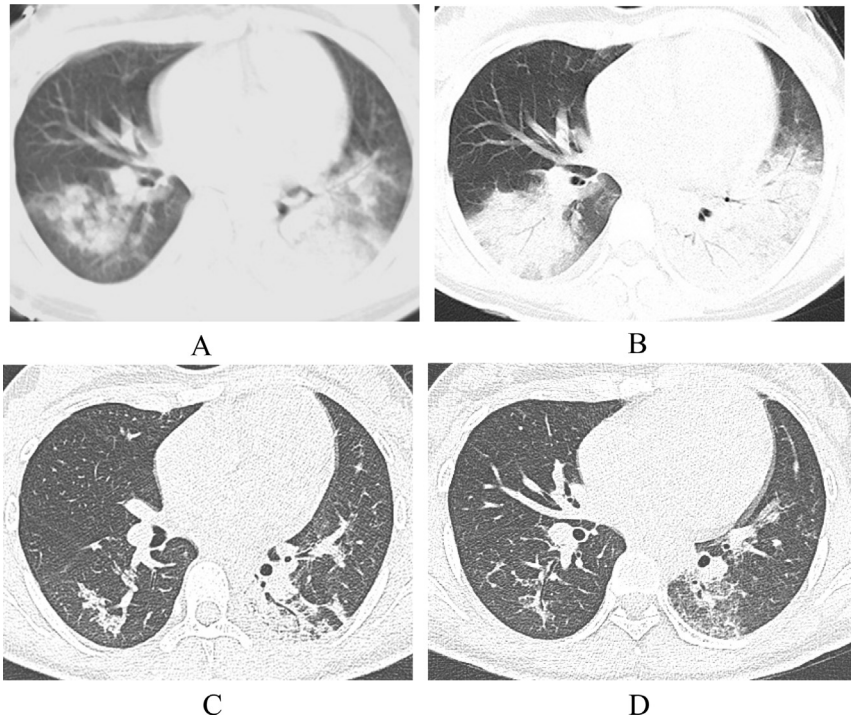

Fig. 2. 20-year-old female patient with H7N9 subtype of human avian influenza. A. MDCT obtained at d 3 after onset shows lobar consolidation in left lung and nodular consolidation in right lung. B. MDCT obtained at d 2 after A shows lobar and segmental consolidation with air bronchogram in both lower lobes. C. MDCT obtained at d 10 after B shows that the extent and density of the lesions obviously decrease. D. MDCT obtained at d 12 after C shows reticulation shadows in both lower lobes.

Netherlands [3,4]. To our knowledge, this is the first time that H7N9 subtype has infected human and caused death. Preliminary studies have shown that the H7N9 subtype of avian influenza virus is novel reassortants and more virulent in humans than other H7 viruses [4,5].

Infection of H7N9 subtype of avian influenza virus typically manifests itself as flulike symptoms such as fever, cough, sore throat, headache and body aches [1,6]. The clinical findings of the 11 patients from our group that had been confirmatively diagnosed as infection of H7N9 subtype of avian influenza virus reveal that rapid progress is characteristic of this disease. A high incidence of severe pneumonia is a common abnormality, with all eleven patients suffering from persistent fever (body temperature of 39 °C or above), and accompanying dyspnea or ARDS. WBC count may be normal or slightly decrease [2].

In our study, the pulmonary lesions of H7N9 infection of human avian influenza were radiologically demonstrated to be segmental or lobar GGO or consolidation combined with air bronchogram at the initial stage without a predominant distribution, which are inconsistent with findings from previous studies [7]. We believe that the pathological mechanism of infection of H7N9 subtype of avian influenza virus may resemble to other viral pneumonia and is based on alveolar exudation. The lesions can develop into either multiple or diffuse at both lungs with rapid progress at the progressive stage, or reticulation when the abnormalities improve later into the later stage (after 20 days) [5,6]. According to the evolution process by radiology, infection of H7N9 subtype of avian influenza virus can be divided into three stages. The initial stage is the first 3 days after onset. The progressive stage is the period of d 3-15 after onset. Period since d 15 after onset is defined as the stable stage. The stable stage is protracted for some cases due to the remaining viral infection in addition with bacterial infections. Pleural effusions are rarely seen and lymph node enlargement is not significant.

The imaging demonstrations of H7N9 subtype infection of avian influenza virus may resemble to other pneumonia including novel swine influenza A (H1N1) virus (S-OIV) infection, severe acute respiratory syndromes (SARS), bacterial pneumonia and highly pathogenic H5N1 subtype human avian influenza virus infection. The main imaging findings of S-OIV infection and SARS are unilateral or bilateral GGO or focal areas of consolidations with a predominant peribronchovascular and subpleural distribution [8−10], while H7N9 subtype avian influenza infection presents pulmonary segment or lobar exudative lesions without obvious distinctive distribution. Bacterial pneumonia usually shows lobar consolidation and increased WBC clinically, which can recover quickly by antibiotic therapy. The imaging findings of H7N9 subtype infection of avian influenza virus resemble to those of H5N1 subtype infection of avian influenza virus, both of which have pulmonary segment or lobar exudative lesions as the predominant imaging findings except that multifocal consolidations have a predilection at lower lobes in cases of H5N1 subtype infection of avian influenza virus [11].

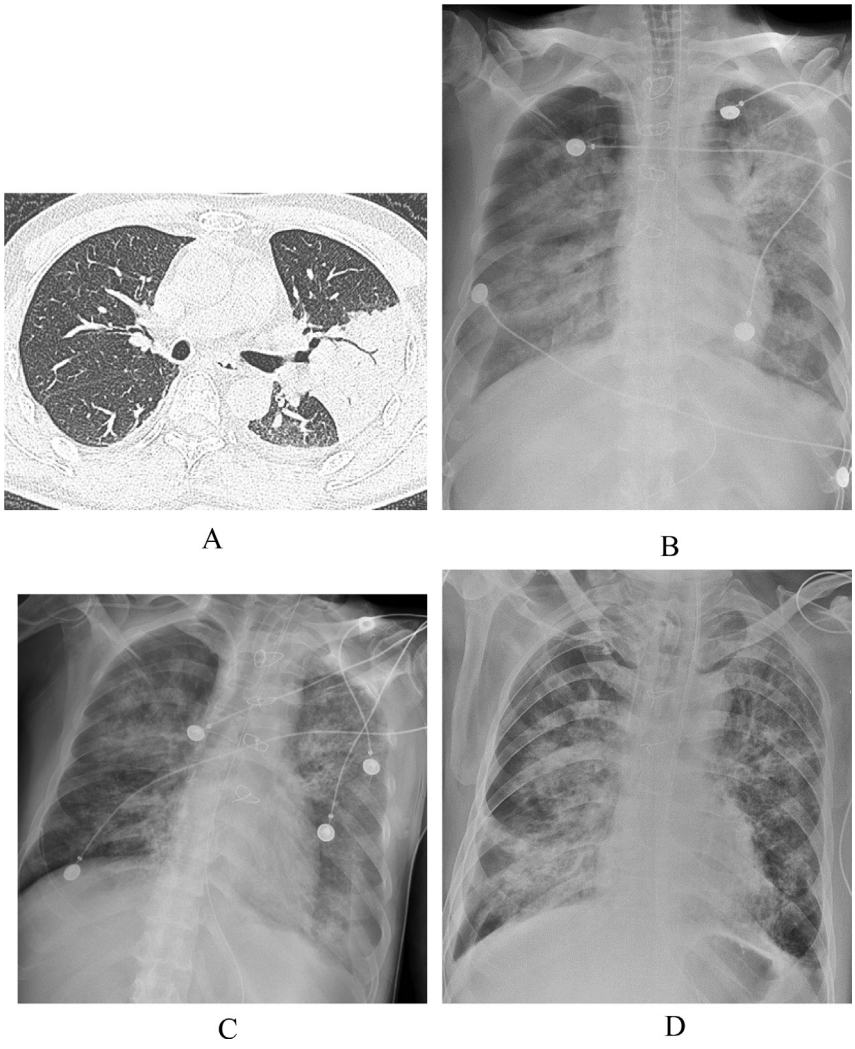

Fig. 3. 56-year-old male patient with H7N9 subtype of human avian influenza and a medical history of excision of thymoma. A. MDCT obtained at d 6 after onset immediately shows lobar consolidation with air bronchogram in upper lobe of left lung. B. Bedside chest radiograph obtained at d 6 after A shows diffuse consolidation and ground-glass opacities in both lung. C. Bedside chest radiograph obtained at d 5 after B shows improved abnormalities, especially in the right lower lobe. D. Bedside chest radiograph obtained at d 18 after C shows progress of the abnormalities in the right lower lobe and reticulation shadows in left lung.

However, differential diagnosis relies on virus isolation and detection [6].

This study has several limitations. Firstly, it is a retrospective study based on a series of 11 cases. Secondly, none of the patients underwent lung biopsy or autospy that allowed radiographics−histopathologic correlation.

In summary, the imaging findings of H7N9 subtype infection of avian influenza virus in this series of patients tends to be pulmonary segment or lobar consolidation and mostly progress rapidly into diffuse exudation.

Financial disclosure

The authors have no financial interests related to the present manuscript.

Funding support

This work was supported by The National Natural Science Foundation of China(No: 81171393 ; 31271066); A Project Funded by the Priority Academic Program Development ofJiangsu Higher Education Institutions (PAPD).

Acknowledgments

This study was supported by The National Natural Science Foundation of China (81171393, 31271066); A Project Funded by the Priority Academic Program Development of Jiangsu Higher Education Institutions (PAPD).

References

[1] Chen Y, Liang W, Yang S, Wu N, Gao H, Sheng J, et al. Human infections with the emerging avian influenza A H7N9 virus from wet market poultry: clinical analysis and characterisation of viral genome. Lancet 2013;381(9881):1916−25.

[2] Guan Y, Farooqui A, Zhu H, Dong W, Wang J, Kelvin DJ. H7N9 Incident, immune status, the elderly and a warning of an influenza pandemic. J Infect Dev Ctries 2013;7(4):302−7.

[3] Liu D, Shi W, Shi Y, Wang D, Xiao H, Li W, et al. Origin and diversity of novel avian influenza A H7N9 viruses causing human infection:

phylogenetic, structural, and coalescent analyses. Lancet 2013;381(9881):1926−32.
[4] Li Q, Zhou L, Zhou M, Chen Z, Li F, Wu H, et al. Epidemiology of human infections with avian influenza A (H7N9) virus in China. N Engl J Med 2014;370(6):520−32.
[5] Gao R, Cao B, Hu Y, Feng Z, Wang D, Hu W, et al. Human infection with a novel avian-origin influenza A (H7N9). Virus. N Engl J Med 2013;368(20):1888−97.
[6] Gao HN, Lu HZ, Cao B, Du B, Shang H, Gan JH, et al. Clinical findings in 111 cases of influenza A (H7N9) virus infection. N Engl J Med 2013;368(24):2277−85.
[7] Wang Q, Zhang Z, Shi Y, Jiang Y. Emerging H7N9 influenza A (novel reassortant avian-origin) pneumonia: radiologic findings. Radiology 2013;268(3):882−9.
[8] Ajlan AM, Quiney B, Nicolaou S, Müller NL. Swine-origin influenza A (H1N1) viral infection: radiographic and CT findings. AJR Am J Roentgenol 2009;193(6):1494−9.
[9] Ooi GC, Daqing M. SARS: radiological features. Respirology 2003;(Suppl.):S15−9.
[10] Wang R, Sun H, Song L, Song W, Cui H, Li B, et al. Plain radiograph and CT features of 112 patients with SARS in acute stage. Beijing Da Xue Xue Bao 2003;35(Suppl.):29−33.
[11] Bay A, Etlik O, Oner AF, Unal O, Arslan H, Bora A, et al. Radiological and clinical course of pneumonia in patients with avian influenza H5N1. Eur J Radiol 2007;61(2):245−50.